Langmuir

Article

pubs.acs.org/Langmuir

Physicochemical Analysis from Real-Time Imaging of Liposome Tubulation Reveals the Characteristics of Individual F-BAR Domain Proteins

Yohko Tanaka-Takiguchi,[†,▽] Toshiki Itoh,[‡] Kazuya Tsujita,[§] Shunsuke Yamada,[†] Miho Yanagisawa,[∥] Kei Fujiwara,[⊥] Akihisa Yamamoto,[#] Masatoshi Ichikawa,[#] and Kingo Takiguchi*[,†]

[†]Division of Biological Science, Graduate School of Science, Nagoya University, Nagoya 464-8602, Japan

[‡]Division of Membrane Biology and [§]Division of Lipid Biochemistry, Department of Biochemistry and Molecular Biology, Kobe University Graduate School of Medicine, Kobe 650-0017, Japan

[∥]Department of Physics, Faculty of Science, Kyushu University, Fukuoka 812-8581, Japan

[⊥]Molecular Robotics Laboratory, Department of Bioengineering and Robotics, Graduate School of Engineering, Tohoku University, Sendai 980-8579, Japan

[#]Physics Department, Graduate School of Science, Kyoto University, Kyoto 606-8502, Japan

Supporting Information

ABSTRACT: The Fer-CIP4 homology-BAR (F-BAR) domain, which was identified as a biological membrane-deforming module, has been reported to transform lipid bilayer membranes into tubules. However, details of the tubulation process, the mechanism, and the properties of the generated tubules remain unknown. Here, we successfully monitored the entire process of tubulation and the behavior of elongated tubules caused by four different F-BAR domain family proteins (FBP17, CIP4, PSTPIP1, and Pacsin2) using direct real-time imaging of giant unilamellar liposomes with dark-field optical microscopy. FBP17 and CIP4 develop many protrusions simultaneously over the entire surface of individual liposomes, whereas PSTPIP1 and Pacsin2 develop only a few protrusions from a narrow restricted part of the surface of individual liposomes. Tubules formed by FBP17 or CIP4 have higher bending rigidities than those formed by PSTPIP1 or Pacsin2. The results provide striking evidence that these four F-BAR domain family proteins should be classified into two groups: one group of FBP17 and CIP4 and another group of PSTPIP1 and Pacsin2. This classification is consistent with the phylogenetic proximity among these proteins and suggests that the nature of the respective tubulation is associated with biological function. These findings aid in the quantitative assessment with respect to manipulating the morphology of lipid bilayers using membrane-deforming proteins.

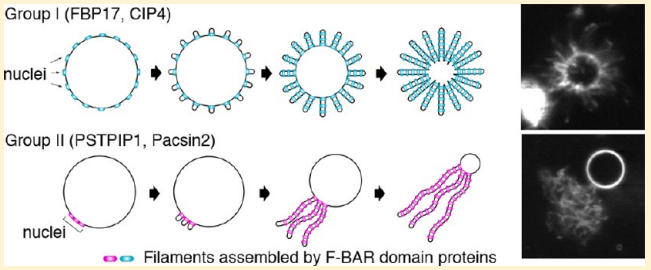

1. INTRODUCTION

The transformation of cell membranes is an essential process for various biological activities, such as cytokinesis, cell motility, endocytosis, exocytosis, and maintaining the functions of organelles in living cells. The basic structure of the cell membrane is a lipid bilayer, and a number of membrane-associated proteins are involved in various biological activities. The F-BAR domain protein family consists of more than 10 different proteins, which have been reported to play important roles in the regulation of cell membranes including the endocytic machinery and cargo selection.[1−3] Proteins belonging to this family (F-BAR proteins) always have an F-BAR domain at their N terminus (Figure S1). Both in vivo and in vitro studies have shown that the F-BAR domain associates on the surface of lipid bilayer membranes.[4−14] Upon associating with a membrane, F-BAR domains spontaneously assemble into spiral or ringed filaments that result in the deformation of the membrane into tubules. Respective F-BAR proteins have unique domains (e.g., Src homology domain 3 (SH3 domain)) at their C termini. The C-terminus region of each F-BAR protein determines its interacting partner(s) and spatiotemporally coordinates its function.[15−21] Thus, differences among the physiological roles of individual F-BAR proteins have been attributable to their C termini. On the other hand, differences among the N-termini of F-BAR domains are not yet well characterized, except that each F-BAR domain produces tubules with a characteristic radius.[6−17] Image analyses by electron microscopy (EM) of the tubules have revealed that the curvature of the crescent-shaped structure of the F-BAR domain determines the diameter of the tubule produced.[22,23]

Received: September 29, 2012
Revised: November 30, 2012
Published: November 30, 2012

However, the dynamic properties of tubulation induced by F-BAR proteins have been little discussed. For this point, in vitro experiments using cell-sized liposomes, along with previous studies,[24−30] have a great potential to determine the dynamic properties of the functions of F-BAR proteins.

Here, we monitored the entire tubulation processes of individual giant unilamellar liposomes (diameter ≥ 3 μm) induced by four distinct F-BAR proteins: FBP17, CIP4, PSTPIP1, and Pacsin2. The behaviors of the membrane tubules generated were analyzed through real-time imaging in a dark-field optical microscope. Real-time images and analyses of physical and chemical parameters exhibit clear differences among the tubulation activities of the groups of FBP17 and CIP4 and those of PSTPIP1 and Pacsin2, in accordance with their phylogenetic proximity. These results raise the possibility that differences in the physicochemical properties of F-BAR domain-induced tubulation itself contribute to the diverse physiological functions of F-BAR proteins. The dynamic measurement of the tubulation induced by various F-BAR domains opens a new perspective in their interactions with the membrane.

2. MATERIALS AND METHODS

2.1. F-BARs. *2.1.1. DNA Constructs.* Each cDNA fragment was subcloned into pGEX6P-1 (GE-Healthcare, Little Chalfont, U.K.). cDNAs encoding human FBP17, CIP4, Pacsin2, and mouse PSTPIP1 were obtained by PCR from a human or mouse brain cDNA using primer sets designed according to database sequences. The following partial constructs were PCR amplified and subcloned into expression vectors: GST-FBP17 F-BAR domain (amino acids 1−300), GST-CIP4 F-BAR domain (amino acids 1−300), GST-Pacsin2 F-BAR domain (amino acids 1−324), and GST-PSTPIP1 F-BAR domain (amino acids 1−300).

2.1.2. Protein Purification and Recombinant Proteins. All recombinant proteins were obtained from bacterial expression systems, according to the manufacturer's instructions (Figure S2). The GST tag of proteins used in the liposome deformation assays was always removed by means of on-bead cleavage with PreScission proteases (GE Healthcare, Little Chalfont, U.K.), and the released proteins were dialyzed in buffer (25 mM Hepes-NaOH, pH 7.4, 100 mM NaCl, and 5 mM EDTA).

2.1.3. Phylogenetic Analysis. The rooted phylogenetic tree of the F-BAR domain of FBP17, CIP4, PSTPIP1, and Pacsin2 proteins was produced by neighbor-joining methods of MEGA 4.[31] Homologues of F-BAR domains were obtained through a BLAST search with 300 amino acid residues at the N terminus of FBP17, CIP4, PSTPIP1, and Pacsin2 of *Homo sapiens* against the genome of each organism.

2.2. Giant Liposomes. *2.2.1. Preparation.* Giant liposomes were prepared using extracted phospholipids as described previously.[26] Phospholipids, phosphatidic acid (PA) from egg yolk, phosphatidylcholine (PC) from egg yolk, phosphatidylethanolamine (PE) from bovine brain, phosphatidylinositol (PI) from soybean or bovine liver, and phosphatidylserine (PS) from bovine brain were purchased from Sigma (St. Louis, MO), and PI from bovine liver was purchased from Avanti Polar Lipids (Alabaster, AL). These lipids were used without further purification. In the case of binary liposomes used, phase separation of lipids is not triggered because of the electrostatic repulsion among charged lipids such as PI and also the great variety in the transition temperature of their fatty acid tails of extracted lipids. In brief, 10 mM phospholipid stock solutions in chloroform/methanol (98:2 v/v) were mixed. The liposome compositions examined were PC and PI, PS, PA, or PE (1:1 mol/mol). The solvent was evaporated under a flow of nitrogen gas, and the lipids were further dried in vacuo for at least 90 min. The dried lipid films were hydrated with 250 mM sucrose at 50 °C for 120 min, and the liposome suspensions were diluted 20-fold with buffer A (25 mM HEPES-NaOH, pH 7.4, 100 mM KCl). The osmolarities of solutions used were measured with a Fiske one-ten osmometer (Advanced Instruments Inc., Norwood, MA). The osmolarities of the sucrose and buffer A solutions are ∼260 and ∼220 mOsm/kg, respectively. The osmotic pressure of inner media of the liposomes (only sucrose) was slightly higher than that of outer media (mixture of sucrose and buffer A solutions), and thus the hypotonic environment maintained their shapes as spherical.

2.2.2. Real-Time Observation and Analysis of Liposome Transformation Process. In each experiment, 10 μL of a liposome suspension, where the concentration of phospholipids was 40 μM, were placed in a glass flow cell at 25 °C and were observed using a dark-field microscope (BHF, Olympus, Tokyo, Japan) with an objective lens (HiApo40, Olympus).[26−29] Two microliters of a solution containing each F-BAR sample was placed into a glass flow cell by capillary force and were gently mixed into the liposome suspension. Floating liposomes were manually tracked in focus, and serial images were recorded using an SIT video camera (IR-1000, Dage-MTI, Michigan City, IN). Liposomes labeled with a lipophilic fluorescent dye (DiI-C18, 1:100 w/w, Invitrogen) were observed using a fluorescence microscope (BH2-RFCA, Olympus). We performed all individual observations at least three times independently to confirm the reproducibility.

To determine persistence length and bending modulus, we adapted the methodology proposed by Yamamoto et al.[32] The persistence length is defined as the decay rate of the angle correlation of tangent vectors taken along the tubule as

$$\langle \vec{t}(s)\cdot\vec{t}(s+\Delta s)\rangle = \exp\left(-\frac{\Delta s}{l_p}\right) \quad (1)$$

where Δs is the distance measured along the tubule between two unit tangent vectors. The bending free energy of the backbone of a tubule can be represented using l_p by regarding the tubule as a polymer chain, while that of the membrane can be represented using κ and then comparing those free energies with respect to the quadratic terms of the radius of curvature of the backbone, where the bending modulus is represented as

$$\kappa = \frac{k_B T l_p}{2\pi r} \quad (2)$$

where r is the radius of the tubule.

2.2.3. Electron Microscopy. Solutions containing liposomes and each F-BAR sample were mixed and preobserved by dark-field microscopy to confirm the liposomal morphology. Optionally, some samples were treated with 2% glutaraldehyde. The mixtures were then applied to glow-discharged collodion- and carbon-coated copper grids, which were stained with 2% uranyl acetate. In each step, excess solution was removed using filter paper. Dried grids were examined using a transmission electron microscope (JEOL Ltd., Tokyo, Japan).

The diameters of tubules were estimated from electron microscope images using ImageJ software. Because the electron micrographs of the membrane tubules were obtained from samples dried on a TEM grid, we estimated that the originally cylindrical tubules have collapsed. Thus, the diameter of the tubule (D) is obtained as $D = W \times {}^{2}/_{\pi}$, where W is the width of the ghost tubule dried and collapsed on the EM grid.

3. RESULTS

3.1. Real-Time Imaging of F-BAR-Induced Tubulation. To investigate the differences among F-BAR proteins, we monitored tubulation produced by four different F-BAR proteins (FBP17, CIP4, PSTPIP1, and Pacsin2 (Figures 1 and S1)) using real-time imaging with a dark-field optical microscope. Dark-field microscopy does not require any labeling for the observation of giant liposomes, meaning that real-time imaging can be used for noninvasive long-term observations and measurements rather than general methods, such as fluorescent labeling.[26−30]

dx.doi.org/10.1021/la303902q | Langmuir 2013, 29, 328−336

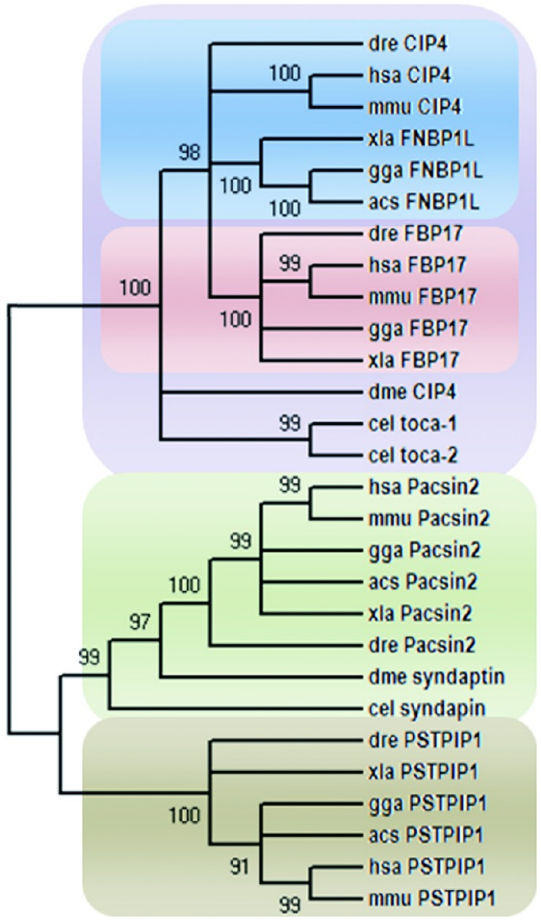

Figure 1. Rooted phylogenetic tree of F-BAR domain proteins from nematoda (*Caenorhadbitis elegans*, cel), fly (*Drosophila melanogaster*, dme), zebrafish (*Danio rerio*, dre), frog (*Xenopus laevis*, xla), green anole (*Anolis carolinensis*, acs), chicken (*Gallus gallus*, gga), mouse (*Mus musculus*, mmu), and human (*Homo sapiens*, hsa). The NCBI-gene IDs are the following: FBP17 – zebrafish 558990, frog 444253, chicken 417187, mouse 14269, human 23048; CIP4 – fly 38534, zebrafish 492762, mouse 106628, human 9322; FNBP1L – frog 446802, lizard 100559983, chicken 424495; toca-1 – nematoda 180492; toca-2 – nematoda 176812; PSTPIP1 – zebrafish 571331, frog 447609, lizard 100566825, chicken 415349, mouse 19200, human 9051; Pacsin2 – zebrafish 404601, frog 398138, lizard 100558017, chicken 395975, mouse 23970, human 11252; and syndapin – nematoda 181058, fly 42467. The tree was prepared by the neighbor joining method, and the local bootstrap probability through 1000 bootstraps is shown above each branch.

To prepare liposomes, we used a two-lipid component system consisting of a representative neutral phospholipid (PC) and an acidic phospholipid (PI, PS, or PA (1:1 mol/mol)) because that model satisfies the conditions for the very simple and highly reproducible preparation of spherical giant unilamellar liposomes.[26−28] Preliminary experiments revealed that all F-BAR domains and proteins (SDS-PAGE analysis is shown in Figure S2) were able to induce tubulation in giant liposomes made from PC and PI, PS, or PA and that substitutions among PI, PS, and PA in the lipid composition did not affect the tubulation (Figure S3). Therefore, for this study, we used PCPI liposomes, which are giant liposomes made from PC and PI (1:1 mol/mol, the same lipid composition used in our previous study).[26]

In this study, the F-BAR domain region of each F-BAR protein (FBP17 F-BAR, CIP4 F-BAR, or PSTPIP1 F-BAR), except Pacsin2, was used for real-time imaging of the tubulation process (Figure S2). It should be noted here that, in the cases of FBP17, CIP4, and PSTPIP1, the liposomal tubulation process induced by the full-length protein and that induced by its F-BAR domain region alone were indistinguishable from each other. When only the F-BAR domain region of Pacsin2 (Pacsin2 F-BAR) was added to giant liposomes, the liposomes collapsed into smaller condensed spheres (Figure S4). Even if liposomes formed tubules, the formed tubules were promptly entangled into the condensing sphere part. However, when full-length Pacsin2 (Pacsin2 full-length) was added to giant liposomes, only tubulation, but not any other transformation, took place. Thus, in the case of Pacsin2, the full-length protein was used.

3.1.1. Tubulation Induced by FBP17 F-BAR. When FBP17 F-BAR was added to the giant liposomes, usually tens of tubules developed simultaneously over the entire surface of each liposome (Figure 2 and Movie S1) and the spherical part of the liposome became smaller as the tubules were elongated (Figure S5). When 4 μM or higher concentrations of FBP17 F-BAR were perfused, the entire part of most liposomes finally changed to asterlike structures composed of many tubules (Figure 3 and Movie S2). If the concentration of added FBP17 F-BAR was insufficient, the elongation of the tubular parts stopped and the unconsumed spherical part of the liposome remained. The entire structure of each liposome was homogeneously labeled with DiI-C18, a lipophilic dye, which indicates that the tubules induced were continuous protrusions from the liposomes (Figure 4).

3.1.2. Tubulation Induced by CIP4 F-BAR. When CIP4 F-BAR was added, many tubules developed simultaneously over the entire surface of each liposome (Figure 2 and Movie S3). After the tubulation, the liposomes finally transformed to asterlike structures composed of many tubules (Figure 3 and Movie S4). This CIP4 F-BAR-induced liposomal tubulation process was indistinguishable from that induced by FBP17 F-BAR, which is consistent with the fact that FBP17 and CIP4 belong to the same subfamily (CIP4 subfamily) (Figure 1).[6]

3.1.3. Tubulation Induced by PSTPIP1 F-BAR. When PSTPIP1 F-BAR was added to the giant liposomes, one or a few tubules developed and were continuously elongated from a restricted point on the surface of each liposome (Figure 2 and Movie S5). The diameter of the spherical part of each liposome became smaller as the tubules were elongated (Figure S5). When 2 μM or higher concentrations of PSTPIP1 F-BAR were perfused, eventually most liposomes were entirely transformed into long tubules, in contrast to the asterlike structures induced by FBP17 F-BAR or CIP4 F-BAR (Figure 3 and Movie S6). If the concentration of PSTIP1 F-BAR added was insufficient, the elongation of the tubular parts stopped and the unconsumed spherical part of the liposome remained. The tubular part was homogeneously labeled with lipophilic dye DiI-C18, similar to the spherical part, indicating that the tubules were continuous protrusions from the liposomes (Figure 4). In the case of PSTPIP1 F-BAR, the process of liposomal tubulation showed an obviously different pattern from the cases of FBP17 F-BAR and CIP4 F-BAR, which is consistent with the fact that PSTPIP1 belongs to a phylogenetically different subfamily than FBP17 and CIP4 (Figure 1).

3.1.4. Tubulation Induced by Pacsin2. When Pacsin2 was added, one or a few tubules developed and were continuously

dx.doi.org/10.1021/la303902q | *Langmuir* 2013, 29, 328−336

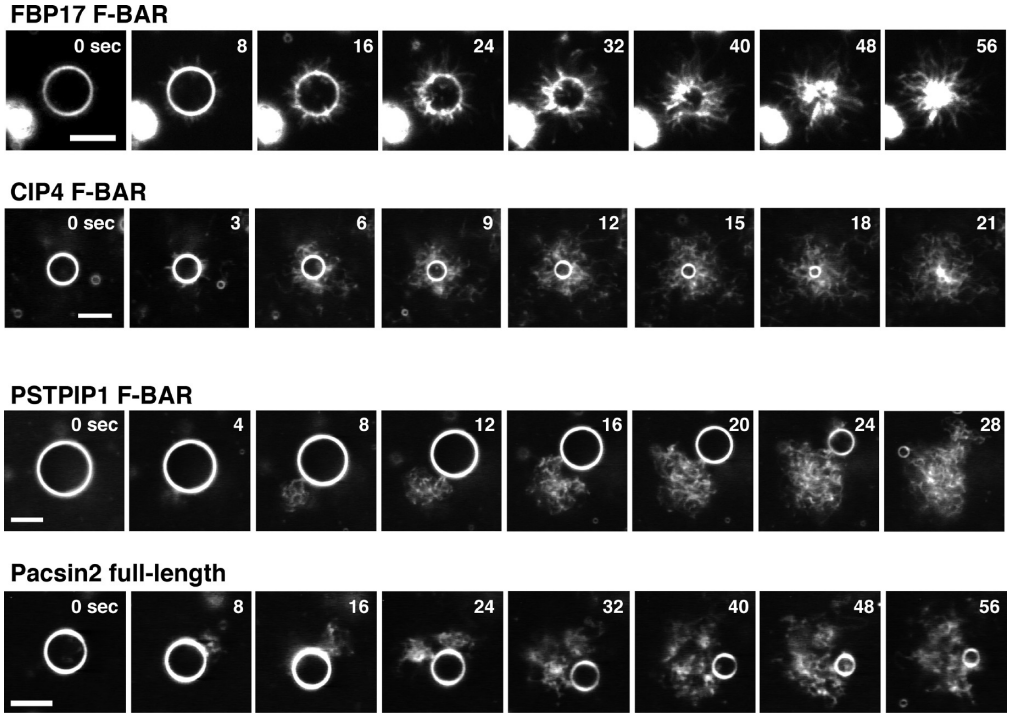

Figure 2. Tubulation process of giant liposomes induced by FBP17 F-BAR, CIP4 F-BAR, PSTPIP1 F-BAR, and Pacsin2 full-length. Time-lapse dark-field images showing the tubulation process induced by each F-BAR protein. FBP17 F-BAR, CIP4 F-BAR, PSTPIP1 F-BAR, or Pacsin2 full-length, added to PCPI liposomes, are indicated for each sequence. The time after the start of tubulation is denoted in seconds in each panel. Bars indicate 10 μm. See also Movies S1, S3, S5, and S7. The final concentrations of FBP17 F-BAR, CIP4 F-BAR, PSTPIP1 F-BAR, and Pacsin2 full-length were 4.7, 4.2, 5.7, and 8.8 μM, respectively. We have confirmed that changes in the concentration of added protein do not cause any essential changes in the characteristics of the tubulation process induced and the tubules formed by each F-BAR protein in the present study (Figure S9 for example).

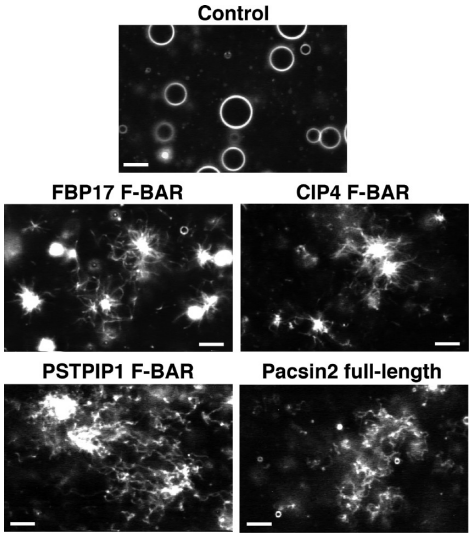

Figure 3. Dark-field micrographs of membrane tubules after the liposomal deformation. PCPI liposomes after the perfusion of buffer A alone (control) and membrane tubules formed by FBP17 F-BAR, CIP4 F-BAR, PSTPIP1 F-BAR, or Pacsin2 full-length are shown. See also Movies S2, S4, S6, and S8. Bars indicate 10 μm. The final concentrations of FBP17 F-BAR, CIP4 F-BAR, PSTPIP1 F-BAR, and Pacsin2 full-length were 4.7, 4.2, 5.7, and 8.8 μM, respectively.

elongated from a restricted point on the surface of each liposome (Figure 2 and Movie S7). After the tubulation, the liposomes finally transformed to long tubules (Figure 3 and Movie S8). This tubulation process was very similar to that induced by PSTPIP1 F-BAR and was clearly different from both cases of FBP17 F-BAR and CIP4 F-BAR. This result is consistent with the fact that the Pacsin2 subfamily is different from the others described above but is phylogenetically near the PSTPIP1 subfamily (Figure 1).

3.2. Ultrastructural Analysis of the Formed Membrane Tubules. The thickness or shape of membrane tubules formed by the F-BAR protein is an important parameter derived from the specificity of each F-BAR domain, and many studies have investigated the thickness.[6−17] Moreover, as described in the following sections, the thickness must be known to evaluate the time-dependent tubulation progress and to investigate the bending elasticity of the tubule formed. For these reasons, the structures of tubules formed by FBP17 F-BAR, CIP4 F-BAR, PSTPIP1 F-BAR, and Pacsin2 were investigated in detail by EM (Figure 5A,B) to determine their thickness, meaning the diameter $2r$ of tubules (Figures 5C and S6). The results indicate that FBP17 F-BAR, CIP4 F-BAR, PSTPIP1 F-BAR, and Pacsin2 formed thinner tubules, in that order. It should be noted that samples of transformed liposomes were preobserved by dark-field microscopy and were then negatively stained for EM observation.

Because the atomic structures of the F-BAR domain regions of FBP17, CIP4, and Pacsin2 but not yet PSTPIP1 have already been solved, the radius of curvature of their membrane-associating interfaces can be calculated from the solved crescent-shaped structures (Figure S7). The calculated radius of curvature for each protein was approximately homologous to the measured radius of the tubules measured through EM observations (Figure 5C), indicating that the curved shape of the F-BAR domain is correlated to the thickness of the tubule, as reported previously.[6−17] Interestingly, the thickness that is

dx.doi.org/10.1021/la303902q | *Langmuir* 2013, 29, 328−336

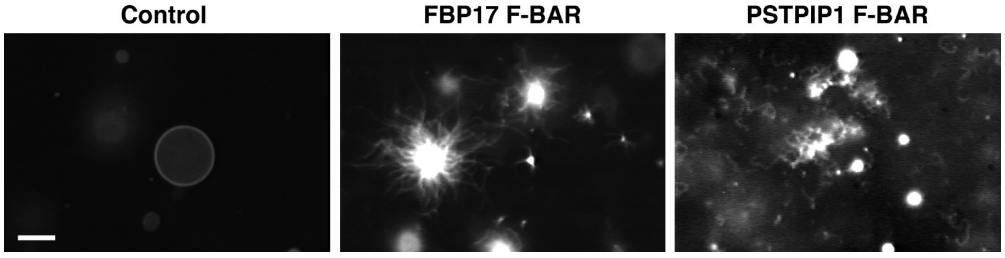

Figure 4. Fluorescent images of liposome membranes labeled with a lipophilic dye, DiI-C18. From left to right, a liposome without F-BAR protein (control) and membrane tubules formed by FBP17 F-BAR and PSTPIP1 F-BAR, respectively. The bar indicates 10 μm. The final concentrations of FBP17 F-BAR and PSTPIP1 F-BAR were 4.7 and 5.7 μM, respectively.

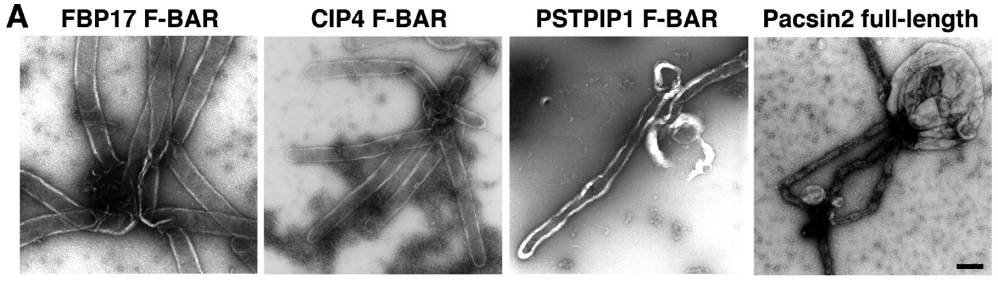

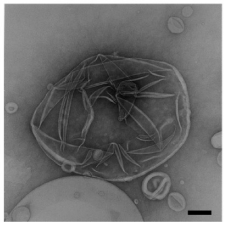

C

	FBP17	CIP4	PSTPIP1	Pacsin2
Thickness of tubules	49 ± 4	36 ± 3	34 ± 3	18 ± 2
Radius of curvature	36	28	N/A	18

Figure 5. Ultrastructure and characteristics of the tubules formed. (A) Electron micrographs of tubules induced by each F-BAR protein. From left to right, FBP17 F-BAR, CIP4 F-BAR, PSTPIP1 F-BAR, and Pacsin2 full-length were added to PCPI liposomes, respectively. The bar indicates 100 nm. As demonstrated by dark-field microscopy, uniform tubules appeared to extend at the expense of the central spherical portion also in the ultrastructural images. Otherwise, the entire surface was tubulated and the transformation reaction was saturated. Higher-magnification images of EM are shown in Figure S10. (B) Representative electron micrograph of a liposome without F-BAR protein (control). The bar indicates 100 nm. (C) Thickness of tubules (half-width, nm) induced by each F-BAR protein (top row = mean ± SD; n = 167, 165, 90, and 75 for FBP17 F-BAR, CIP4 F-BAR, PSTPIP1 F-BAR, and Pacsin2 full-length, respectively), which was estimated from the width of the ghosts collapsed on EM grids. The distribution of the tubule diameters ($2r$) is shown in Figure S6. In the bottom row, the radius of curvature (nm) of the membrane-associating interface of the F-BAR domain region of each F-BAR protein, which was calculated from the already-solved atomic structure, is shown. In the case of PSTPIP1 F-BAR, the radius of curvature is not determined because the atomic structure is not yet solved (N/A).

actually measured is slightly larger than that estimated from the atomic structure, which is probably due to the elastic resistance of the lipid bilayer membrane against deformation.

3.3. Quantitative Analysis of the Tubulation Process. To determine the quantitative differences between the group of FBP17 and CIP4 and the group of PSTPIP1 and Pacsin2 during the tubulation process, we analyzed the velocity of the tubulation. Although not all tubules are displayed in the movies, we estimated this parameter from the difference in surface area of the central spherical part of the liposome A_c from the initial value A_0. The difference in surface area ΔA (= $A_0 - A_c$) is plotted semilogarithmically against time t in Figure S5 (0 s is defined as the time when we first observed the tubulation). Interestingly, some slopes of $\Delta A-t$ curves were changed to be smaller at a certain time (e.g., A1, 20 s; A3, 15 s; A4, 10 s; B3, 100 s; D2, 100 s; D3, 100 s; D6, 30 s).

To clarify this transition, we assume that the tubulation process is classified into two steps: (step 1) development of a new tubule and elongation of tubules; (step 2) elongation of only N^* tubules. In addition, when the total surface area of the lipid membrane is kept constant throughout the tubulation, the increase in ΔA should reflect the increases in the number N and length l of tubules with a constant thickness of $2r$ (Figures 5 and S6). Under these assumptions, the differences in surface areas for step 1 (ΔA_1) and step 2 (ΔA_2) are expressed by

$$\Delta A_1 = 2\pi N(t)(r^2 + rl(t)) \quad (3)$$

and

$$\Delta A_2 = 2\pi N^*(r^2 + rl(t)) \quad (4)$$

where $N(t)$ and $l(t)$ are the velocities of the development of new tubules and the elongation of tubules, respectively. Using these relationships, we fitted the $\Delta A-t$ curves (Figure S5) and found that the initial tubulation process of most liposomes occurred in step 1 (development of new tubules and elongation of tubules), and some of them were transited to step 2 (only elongation of tubules) when the number of tubules increased to N^*. Some liposomes with only step 2 are likely to have finished step 1 before our observation (Figure S5(B4, B6, C3, and D4)).

dx.doi.org/10.1021/la303902q | Langmuir 2013, 29, 328−336

Accordingly, we obtained the unknown parameters (i.e., the final number of tubules N^* and velocities $N(t)$ and $l(t)$) and compared them among the four different F-BAR proteins (Table 1). As for N^*, FBP17 (N^* ~30) has a similar value to

Table 1. Quantitative Analysis of the Tubulation Process[a]

	FBP17	CIP4	PSTPIP1	Pacsin2
N^*	30 ± 8	20 ± 6	6 ± 4	4 ± 2
$l(t)/N(t)$	1.4 ± 1.3	2.8 ± 1.6	42 ± 29	90 ± 57

[a]The N^* values and the ratio $l(t)/N(t)$ are shown (means ± SD, n = 16, 7, 12, and 6, respectively).

CIP4 (N^* ~20). However, the N^* values for PSTPIP1 (N^* ~6) and Pacsin2 (N^* ~4) are much smaller. It should be mentioned that these analytically obtained N^* values were almost the same as the experimental values. In contrast, the magnitude of the velocity ratio between $l(t)$ and $N(t)$ (i.e., $l(t)/N(t)$) shows an opposite relation between the two groups. The $l(t)/N(t)$ values for FBP17 and CIP4 are 1.4 and 2.8, respectively, whereas $l(t)/N(t)$ for PSTPIP1 and Pacsin2 are more than 15 times larger (i.e., ~42 for PSTPIP1 and ~90 for Pacsin2).

As mentioned above, we succeeded in classifying the F-BAR proteins into two groups from the qualitative analysis of the tubulation process, i.e., the group of FBP17 and CIP4 having large N^* and small $l(t)/N(t)$, and the group of PSTPIP and Pacsin2 having small N^* and large $l(t)/N(t)$. In other words, in the case of FBP17 and CIP4, many tubules develop simultaneously, and the elongation of each tubule proceeds slowly. In contrast, in the case of PSTPIP and Pacsin2, only a few tubules develop, and each tubule elongates promptly.

3.4. Elasticity of the Formed Tubules. Dark-field microscopy yields high contrast images of membranes that allows the observation of the behavior of tiny membrane tubules with several tens of nanometers in diameter below earlier detection limits.[26−30] Thus, we could characterize and compare the physicochemical features of the tubules formed among these four F-BAR proteins. The formed tubules were fluctuating owing to Brownian motion, which reflected the elasticity of the individual tubules or the bending modulus of the membrane. Therefore, we can estimate the bending modulus of the membrane with each F-BAR protein to determine a reinforced effect by the proteins. Figure 6 shows the angle correlations of the tangent vectors taken along the tubules. Note that the slopes of the correlation plot, which correspond to the persistence length (l_p) of each tubule, were grouped. Through the analytical calculation including the thickness of the tubule (Figure 5C), the comparable bending modulus of each membrane with the respective F-BAR protein can be estimated theoretically.[32] Table 2 shows the bending modulus of the membrane of tubules induced by FBP17 F-BAR, CIP4 F-BAR, PSTPIP1 F-BAR, and Pacsin2 (Figure S8). The comparison of the bending modulus indicates that the four F-BAR proteins can be classified into two groups with respect to the bending modulus: FBP17 ($\kappa \approx 40k_BT$) and CIP4 ($\kappa \approx 51k_BT$) reinforced the membrane tubules approximately twice as much as did PSTPIP1 ($\kappa \approx 19k_BT$) and Pacsin2 ($\kappa \approx 25k_BT$). The result of the classification is the same as that determined by the analysis of the tubulation process.

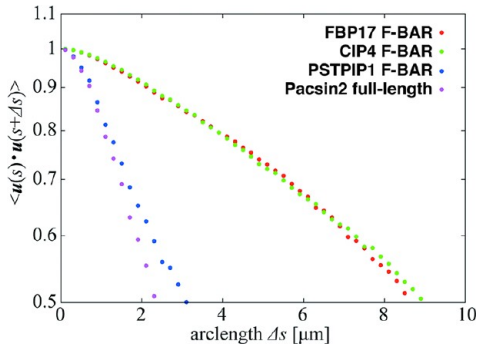

Figure 6. Elasticity of the formed membrane tubules. The angle correlations of the tangent vectors taken along the tubules with the four F-BAR proteins (FBP17 F-BAR, CIP4 F-BAR, PSTPIP1 F-BAR, and Pacsin2 full-length). The persistence length of each tubule is calculated from the slope of the tangent correlation.[32] Calculated l_p values are described in Table 2.

Table 2. Persistence Length (l_p) and Bending Modulus (κ) of the Membrane Reinforced by Four F-BAR Proteins[a]

	FBP17	CIP4	PSTPIP1	Pacsin2
l_p (μm)	12.3 ± 0.2	11.6 ± 0.1	4.0 ± 0.1	2.8 ± 0.0
κ (k_BT)	40.0 ± 2.9	51.3 ± 3.6	18.5 ± 1.7	24.8 ± 2.8

[a]In terms of F-BAR-protein-associated tubules, radii were measured from EM images (Figure 5C), where each l_p is an experimentally determined value, and the bending modulus of the membrane is calculated from eq 3 (mean ± SD, n = 133, 103, 151, and 29, respectively). The tubules formed by PSTPIP1 or Pacsin2 exhibited the same magnitude of the modulus as that with a typical lipid membrane without an F-BAR protein,[39,40] whereas the bending modulus of the tubules formed by FBP17 or CIP4 is several times larger. It should be noted here that to obtain control data we have tried to make tubules from PCPI liposomes under the same experimental conditions as much as possible. However, liposomes never developed tubules, which may be due to the electrical repulsion among PI lipids.

4. DISCUSSION

In this study, we reveal the characteristic of tubulation activity of four different F-BAR proteins and show that they could be classified into two groups. Group I, FBP17 and CIP4, shows the extensive development of many tubules, the slow elongation of tubules, and the formation of hard tubules. Group II, PSTPIP1 and Pacsin2, shows the number- and position-restricted development of tubules, the fast elongation of tubules, and the formation of soft tubules.

This grouping, based on real-time imaging of reconstituted F-BAR proteins, is consistent with that derived through phylogenetic trees (Figure 1). Organisms from nematodes to humans possess a set of F-BAR proteins that belongs to both groups although F-BAR proteins in flies and nematodes have a slightly lower homology. These findings suggest that such partitioning roles among the different groups of F-BAR proteins exist in living cells. However, to conclude that there are functionally distinct groups within the protein family, a larger number of F-BAR proteins should be analyzed in the similar manner.

Tubules formed by group I F-BAR proteins had a higher bending rigidity than those formed by group II F-BAR proteins. Because the rigidity may depend on the density of F-BAR proteins wrapping the tubules, we expect that the proteins of group I are associating with tubules with a higher density than those in group II.

dx.doi.org/10.1021/la303902q | Langmuir 2013, 29, 328−336

Tubulation induced by each F-BAR protein has a regular property; that is, the tubules are induced through a specific tubulation process that is completely different from the random membrane deformations brought about by changing environmental factors such as temperature, osmolarity, and pH.[29,33−35] Thus, these tubules should function optimally to maintain a number of well-ordered membrane trafficking events within living cells, such as endocytosis, exocytosis, and endosomal transport. F-BAR proteins probably maintain the proper functions of cells by inducing tubulation with the appropriate properties.

Our previous studies revealed that the force required for the development of a new tubule is much larger than that required for the elongation of a tubule.[25,30,36] Thus, it is plausible that this process for the development of a new tubule is also crucial to F-BAR-protein-induced tubulation, and its degree may determine the number of tubules generated from each liposome. It has been reported that the assembly of F-BAR domains into membrane-wrapping spiral or ringed filaments induces tubulation.[10,13,16,23,37] Therefore, the development of a new tubule requires the nucleation of F-BAR domains on the membrane surface because nucleation is an indispensable process for the initiation of protein assembly.[38] Taken together, we hypothesize that the process occurs as shown in Figure 7. If the nucleation takes place easily and the nucleation sites diffuse on the membrane freely from each other, then tubules can develop from anywhere on the liposome surface and the number of tubules should increase; that is the case for group I F-BAR proteins. If the elongation takes place at a much higher rate than the nucleation and if the nucleation sites have a tendency to clump between each other, then fewer numbers of tubules can develop from only a restricted part of the liposome; that is the case for group II F-BAR proteins. In the cases of FBP17 and CIP4 (group I), not only the ordinary tip-to-tip but also the lateral interactions between the crescent-shaped F-BAR domains on the membrane surface have been reported.[11] These multiple protein−protein interactions may facilitate the nucleation of the F-BAR proteins of group I. However, the protein−lipid interaction has been unclear. We expect that the difference in balance between these interactions classifies the F-BAR domains into two groups.

In all cases, to elucidate the variety among the protein family, a more detail investigation of the membrane-binding kinetics and the clustering kinetics of these proteins that are involved in the tubulation are essentially important (Figure S9).

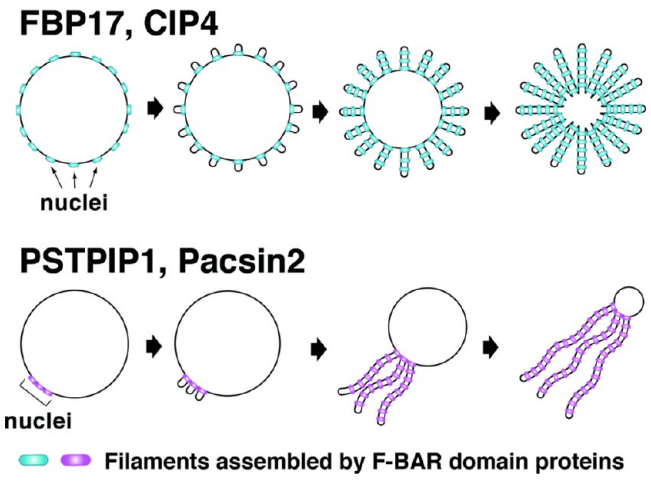

Figure 7. Model for F-BAR protein-induced liposomal tubulation. The model shows schematic representations of the differences found in the process of the F-BAR protein-induced liposomal tubulation. By direct real-time imaging, we demonstrate that the four distinct F-BAR proteins induce tubulation in giant unilamellar liposomes through different processes, and they are classified into two groups. FBP17 and CIP4 develop many projections simultaneously throughout the surface of individual giant liposomes (upper), whereas PSTPIP1 and Pacsin2 develop only a few projections from a narrow restricted surface of individual giant liposomes (bottom). These ensure that a nucleation process is involved in the tubulation (each frame on the left). Membrane-bound FBP17 or CIP4 may assemble into many nuclei everywhere on the membrane surface, whereas membrane-bound PSTPIP1 or Pacsin2 assembles into a single nucleus or a cluster that is made from a few nuclei. F-BAR proteins polymerize to filaments based on such nuclei. The filaments (blue and red ovals) brace and wrap around the membrane, thus membrane projections are developed and elongated.

5. CONCLUSIONS

In this study, continuous real-time imaging of the entire tubulation process of giant liposomes induced by F-BAR proteins and membrane tubules formed as result of the tubulation is performed. Quantitative analyses of that imaging with respect to the number, elongation rate, and elasticity of the tubules show that different F-BAR proteins are able to induce unique tubulations, which is consistent with the evolutional differentiation of the proteins.

■ ASSOCIATED CONTENT

Ⓢ Supporting Information

Real-time observations of liposome suspensions mixed with an F-BAR sample. Schematic presentation of the domain structures of F-BAR domain family proteins FBP17, CIP4, PSTPIP1, and Pacsin2. SDS-PAGE and CBB stain analyses of the F-BAR samples used. Effect of lipid composition on tubulation. Transformation of giant liposomes induced by Pacsin2 F-BAR. Time evolution of the tubulation process. Thickness of the formed tubules as determined by EM. Radius of curvature calculation. Time-dependent progress of the persistence length and bending modulus of the formed membrane tubules. Tubulation activity and membrane affinity of F-BAR. Enlarged images of membrane tubules. This material is available free of charge via the Internet at http://pubs.acs.org.

■ AUTHOR INFORMATION

Corresponding Author

*Tel: +81 52 788 6248. Fax: +81 52 789 3001. E-mail: j46037a@nucc.cc.nagoya-u.ac.jp.

Present Address

▽Structural Biology Research Center, Graduate School of Sciences, Nagoya University, Nagoya 464-8601, Japan.

Notes

The authors declare no competing financial interest.

■ ACKNOWLEDGMENTS

We thank Mr. Toshiaki Gotoh (Technical Center of Nagoya University) for help with the EM, Prof. Kuniaki Nagayama (National Institute for Physiological Sciences, Japan) for his invaluable encouragement, and Prof. Hirokazu Hotani (Nagoya University, Japan) for the critical reading of the manuscript. This work was supported by the MEXT of Japan under a Grant-in-Aid for Scientific Research on Priority Areas "Soft

Matter Physics" (project no. 21015010) and "System Cell Engineering by Multi-Scale Manipulation" (project no. 20034024) and on Innovative Areas "Molecular Robotics" (project no. 24104004), the JSPS under a Grant-in-Aid for Challenging Exploratory Research (project no. 24651134), and the JST/CNRS under a Strategic Japanese-French Cooperative Program on "Structure and Function of Biomolecules" ("Structural Bases of Actin Nucleation in the Vicinity of Membrane", project no. 25-J-J5208).

■ ABBREVIATIONS

EM, electron microscopy; F-BAR, Fer-CIP4 homology-BAR; PA, phosphatidic acid; PC, phosphatidylcholine; PE, phosphatidylethanolamine; PI, phosphatidylinositol; PS, phosphatidylserine

■ REFERENCES

(1) Itoh, T.; De Camilli, P. BAR, F-BAR (EFC) and ENTH/ANTH Domains in the Regulation of Membrane-Cytosol Interfaces and Membrane Curvature. *Biochim. Biophys. Acta* **2006**, *1761*, 897−912.
(2) Takano, K.; Toyooka, K.; Suetsugu, S. EFC/F-BAR Proteins and the N-WASP-WIP Complex Induce Membrane Curvature-Dependent Actin Polymerization. *EMBO J.* **2008**, *27*, 2817−2828.
(3) Itoh, T.; Takenawa, T. Mechanisms of Membrane Deformation by Lipid-Binding Domains. *Prog. Lipid Res.* **2009**, *48*, 298−305.
(4) Fricke, R.; Gohl, C.; Dharmalingam, E.; Grevelhörster, A.; Zahedi, B.; Harden, N.; Kessels, M. M.; Qualmann, B.; Bogdan, S. Drosophila Cip4/Toca-1 Integrates Membrane Trafficking and Actin Dynamics Through WASP and SCAR/WAVE. *Curr. Biol.* **2009**, *19*, 1429−1437.
(5) Fricke, R.; Gohl, C.; Bogdan, S. The F-BAR Protein Family Actin' on the Membrane. *Commun. Integr. Biol.* **2010**, *3*, 89−94.
(6) Heath, R. J. W.; Insall, R. H. F-BAR Domains: Multifunctional Regulators of Membrane Curvature. *J. Cell Sci.* **2008**, *121*, 1951−1954.
(7) de Kreuk, B.-J.; Nethe, M.; Fernandez-Borja, M.; Anthony, E. C.; Hensbergen, P. J.; Deelder, A. M.; Plomann, M.; Hordijk, P. L. The F-BAR Domain Protein PACSIN2 Associates with Rac1 and Regulates Cell Spreading and Migration. *J. Cell Sci.* **2011**, *124*, 2375−2388.
(8) Tsujita, K.; Sasaki, N.; Furutani, M.; Oikawa, T.; Suetsugu, S.; Takenawa, T. Coordination between the Actin Cytoskeleton and Membrane Deformation by a Novel Membrane Tubulation Domain of PCH Proteins Is Involved in Endocytosis. *J. Cell Biol.* **2006**, *172*, 269−279.
(9) Henne, W. M.; Kent, H. M.; Ford, M. G.; Hegde, B. G.; Daumke, O.; Butler, P. J.; Mittal, R.; Langen, R.; Evans, P. R.; McMahon, H. T. Structure and Analysis of FCHo2 F-BAR Domain: A Dimerizing and Membrane Recruitment Module that Effects Membrane Curvature. *Structure* **2007**, *15*, 839−852.
(10) Shimada, A.; Niwa, H.; Tsujita, K.; Suetsugu, S.; Nitta, K.; Hanawa-Suetsugu, K.; Akasaka, R.; Nishino, Y.; Toyama, M.; Chen, L.; Liu, Z. J.; Wang, B. C.; Yamamoto, M.; Terada, T.; Miyazawa, A.; Tanaka, A.; Sugano, S.; Shirouzu, M.; Nagayama, K.; Takenawa, T.; Yokoyama, S. Curved EFC/F-BAR Domain Dimers Are Joined End to End into a Filament for Membrane Invagination in Endocytosis. *Cell* **2007**, *129*, 761−772.
(11) Frost, A.; Roux, A.; Perera, R.; Spasov, K.; Destaing, O.; Egelman, E. H.; De Camilli, P.; Unger, V. M. Structural Basis of Membrane Invagination by F-BAR Domains. *Cell* **2008**, *132*, 807−817.
(12) Guerrier, S.; Coutinho-Budd, J.; Sassa, T.; Gresset, A.; Jordan, N. V.; Chen, K.; Jin, W. L.; Frost, A.; Polleux, F. The F-BAR Domain of srGAP2 Induces Membrane Protrusions Required for Neuronal Migration and Morphogenesis. *Cell* **2009**, *138*, 990−1004.
(13) Shimada, A.; Takano, K.; Shirouzu, M.; Hanawa-Suetsugu, K.; Terada, T.; Toyooka, K.; Umehara, T.; Yamamoto, M.; Yokoyama, S.; Suetsugu, S. Mapping of the Basic Amino-Acid Residues Responsible for Tubulation and Cellular Protrusion by the EFC/F-BAR Domain of Pacsin2/Syndapin II. *FEBS Lett.* **2010**, *584*, 1111−1118.
(14) Henne, W. H.; Boucrot, E.; Meinecke, M.; Evergren, E.; Vallis, Y.; Mittal, R.; McMahon, H. T. FCHo Proteins are Nucleators of Clathrin-Mediated Endocytosis. *Science* **2010**, *328*, 1281−1284.
(15) Itoh, T.; Erdmann, K. S.; Roux, A.; Habermann, B.; Werner, H.; De Camilli, P. Dynamin and the Actin Cytoskeleton Cooperatively Regulate Plasma Membrane Invagination by BAR and F-BAR Proteins. *Dev. Cell* **2005**, *9*, 791−804.
(16) Suetsugu, S. The Proposed Functions of Membrane Curvatures Mediated by the BAR Domain Superfamily Proteins. *J. Biochem.* **2010**, *148*, 1−12.
(17) Rao, Y.; Ma, Q.; Vahedi-Faridi, A.; Sundborger, A.; Pechstein, A.; Puchkov, D.; Luo, L.; Shupliakov, O.; Saenger, W.; Haucke, V. Molecular Basis for SH3 Domain Regulation of F-BAR-Mediated Membrane Deformation. *Proc. Natl. Acad. Sci. U.S.A.* **2010**, *107*, 8213−8218.
(18) Ahmed, S.; Bu, W.; Lee, R. T. C.; Maurer-Stroh, S.; Goh, W. I. F-BAR Domain Proteins. *Commun. Integr. Biol.* **2010**, *3*, 116−121.
(19) Bu, W.; Lim, K. B.; Yu, Y. H.; Chou, A. M.; Sudhaharan, T.; Ahmed, S. Cdc42 Interaction with N-WASP and Toca-1 Regulates Membrane Tubulation, Vesicle Formation and Vesicle Motility: Implications for Endocytosis. *PLoS One* **2010**, *5*, e12153.
(20) Campellone, K. G.; Siripala, A. D.; Leong, J. M.; Welch, M. D. Membrane-Deforming Proteins Play Distinct Roles in Actin Pedestal Biogenesis by Enterohemorrhagic *E. coli*. *J. Biol. Chem.* **2012**, *287*, 20613−20624.
(21) Wakita, Y.; Kakimoto, T.; Katoh, H.; Negishi, M. The F-BAR Protein Rapostlin Regulates Dendritic Spine Formation in Hippocampal Neurons. *J. Biol. Chem.* **2011**, *286*, 32672−32683.
(22) Quan, A.; Xue, J.; Wielens, J.; Smillie, K. J.; Anggono, V.; Parker, M. W.; Cousin, M. A.; Graham, M. E.; Robinson, P. J. Phosphorylation of Syndapin I F-BAR Domain at Two Helix-Capping Motifs Regulates Membrane Tubulation. *Proc. Natl. Acad. Sci. U.S.A.* **2012**, *109*, 3760−3765.
(23) Wang, Q.; Navarro, M. V. A. S.; Peng, G.; Molinelli, E.; Goh, S. L.; Judson, B. L.; Rajashankar, K. R.; Sondermann, H. Molecular Mechanism of Membrane Constriction and Tubulation Mediated by the F-BAR Protein Pacsin/Syndapin. *Proc. Natl. Acad. Sci. U.S.A.* **2009**, *106*, 12700−12705.
(24) Bacia, K.; Futai, E.; Prinz, S.; Meister, A.; Daum, S.; Glatte, D.; Briggs, J. A. G.; Schekman, R. Multibudded Tubules Formed by COPII on Artificial Liposomes. *Sci. Rep.* **2011**, *1*, 17.
(25) Umeda, T.; Inaba, T.; Ishijima, A.; Takiguchi, K.; Hotani, H. Formation and Maintenance of Tubular Membrane Projections: Experiments and Numerical Calculations. *BioSystems* **2008**, *93*, 115−119.
(26) Tanaka-Takiguchi, Y.; Kinoshita, M.; Takiguchi, K. Septin-Mediated Uniform Bracing of Phospholipid Membranes. *Curr. Biol.* **2009**, *19*, 140−145.
(27) Takiguchi, K.; Nomura, F.; Inaba, T.; Takeda, S.; Saitoh, A.; Hotani, H. Liposomes Possess Drastic Capabilities for Topological Transformation. *ChemPhysChem* **2002**, *3*, 571−574.
(28) Nomura, F.; Nagata, M.; Inaba, T.; Hiramatsu, H.; Hotani, H.; Takiguchi, K. Capabilities of Liposomes for Topological Transformation. *Proc. Natl. Acad. Sci. U.S.A.* **2001**, *98*, 2340−2345.
(29) Takeda, S.; Saitoh, A.; Furuta, M.; Satomi, N.; Ishino, A.; Nishida, G.; Sudo, H.; Hotani, H.; Takiguchi, K. Opening of Holes in Liposomal Membranes Is Induced by Proteins Possessing the FERM Domain. *J. Mol. Biol.* **2006**, *362*, 403−413.
(30) Inaba, T.; Ishijima, A.; Honda, M.; Nomura, F.; Takiguchi, K.; Hotani, H. Formation and Maintenances of Tubular Membrane Projections Require Mechanical Force. *J. Mol. Biol.* **2005**, *348*, 325−333.
(31) Tamura, K.; Dudley, J.; Nei, M.; Kumar, S. MEGA4: Molecular Evolutionary Genetics Analysis (MEGA) Software Version 4.0. *Mol. Biol. Evol.* **2007**, *24*, 1596−1599.

(32) Yamamoto, A.; Ichikawa, M. Direct Measurement of Single Soft Lipid Nanotubes: Nanoscale Information Extracted in Noninvasive Manner. *Phys. Rev. E* **2012**, *86*, 061905.
(33) Taniguchi, T.; Yanagisawa, M.; Imai, M. Numerical Investigations of the Dynamics of Two-Component Vesicles. *J. Phys.: Condens. Matter* **2011**, *23*, 284103.
(34) Yanagisawa, M.; Imai, M.; Taniguchi, T. Shape Deformation of Ternary Vesicles Coupled with Phase Separation. *Phys. Rev. Lett.* **2008**, *100*, 148102.
(35) Yanagisawa, M.; Imai, M.; Taniguchi, T. Periodic Modulation of Tubular Vesicles Induced by Phase Separation. *Phys. Rev. E* **2010**, *82*, 051928.
(36) Shitamichi, Y.; Ichikawa, M.; Kimura, Y. Mechanical Properties of a Giant Liposome Using Optical Tweezers. *Chem. Phys. Lett.* **2009**, *479*, 274−278.
(37) Saarikangas, J.; Zhao, H.; Pykalainen, A.; Laurinmaki, P.; Mattila, P. K.; Kinnunen, P. K.; Butcher, S. J.; Lappalainen, P. Molecular Mechanisms of Membrane Deformation by I-BAR Domain Proteins. *Curr. Biol.* **2009**, *19*, 95−107.
(38) Oosawa, F.; Asakura, S. *Thermodynamics of the Polymerization of Protein*; Academic Press: New York, 1975.
(39) Rawicz, W.; Olbrich, K. C.; McIntosh, T.; Needham, D.; Evans, E. Effect of Chain Length and Unsaturation on Elasticity of Lipid Bilayers. *Biophys. J.* **2000**, *79*, 328−339.
(40) Gracià, R. S.; Bezlyepkina, N.; Knorr, R. L.; Lipowsky, R.; Dimova, R. Effect of Cholesterol on the Rigidity of Saturated and Unsaturated Membranes: Fluctuation and Electrodeformation Analysis of Giant Vesicles. *Soft Matter* **2010**, *6*, 1472−1482.

■ NOTE ADDED AFTER ASAP PUBLICATION

This article was published ASAP on December 13, 2012. Reference 32 has been updated. The correct version was published on December 19, 2012.